3-D Scheimpflug Corneal Tomography

Why we need this technology to assess refractive surgery candidates' risk of ectasia.

BY RENATO AMBRÓSIO JR, MD, PHD

One of the most common challenges for any refractive surgeon is to properly identify and address patients at increased risk of ectatic progression. Traditionally, surgeons have used Placido disk-based corneal topography and ultrasound central corneal thickness (CCT) measurements when screening refractive surgery candidates for their risk of ectasia.[1,2]

In addition to topography and CCT, researchers considered the patient's level of correction, residual stromal bed, and age when developing the Ectasia Risk Scoring System,[3] which was later validated.[4] This system originally had 4% to 8% false negatives.[3-5] In a separate retrospective study involving 36 cases of ectasia after LASIK, nine eyes (25%) were classified as low risk.[6] These observations are in agreement with other cases of ectasia after LASIK in the absence of apparent risk factors based on classic screening methods.[7-9] The incidence of false positives is also relatively high among cases that are stable after LASIK.[10] The need for more sensitive and specific tests to evaluate refractive surgery candidates' risk of ectasia is therefore without question.

The advent of corneal tomography (CTm) represents an evolution in corneal analysis.[11] CTm computes a three-dimensional (3-D) image of the cornea, beyond corneal surface topography and CCT. CTm permits the characterization of the front and back surfaces of the cornea, thereby generating a pachymetric map. As with any auxiliary examination, users must have a proper understanding of the fundamental clinical questions related to the need for the complementary data to appreciate the test's relevance. Regarding the role of CTm for screening refractive surgery candidates, it is critical to understand that a susceptibility to ectasia (often referred to as *forme fruste keratoconus*) usually occurs in eyes with relatively normal front-surface topography. In these cases, an abnormal back elevation and pachymetric distribution provide evidence that the tomographic characterization enhances the sensitivity of this approach for detecting a predisposition to ectasia.[12]

3-D ROTATIONAL SCHEIMPFLUG CORNEAL AND ANTERIOR SEGMENT TOMOGRAPHY

Oculus Optikgeräte GmbH (Wetzlar, Germany) introduced the Pentacam Comprehensive Eye Scanner in 2002 as the first corneal and anterior segment tomography system using digital rotating Scheimpflug photography. Initially described by Jules Carpentier in 1901, the Scheimpflug principle is a geometric rule commonly used in photography to enhance the depth of focus without significantly distorting the image. Carpentier's innovative work was cited and credited in the original patent by Theodor Scheimpflug in 1904. In this technique, the three imaginary planes (the film plane, the lens plane, and the plane of sharp focus) are disposed in a nonparallel manner.

Twenty-five to 50 Scheimpflug images are acquired during one scan for a 3-D tomographic reconstruction with the Pentacam. A second frontal pupillary camera aligns the images and compensates for ocular movement. The device calculates a quality specification score, which takes into account the area covered, alignment, and ocular motion. This score helps users assess the validity of the data in each examination.

INTERPRETATION OF CORNEAL TOMOGRAPHY

The interpretation of color-coded topographic and tomographic maps for clinical decisions is a relatively complex and confusing task. Users must have a basic knowledge of the type of maps that are evaluated in order to carefully and consciously choose the color-coded scale for each map.

CURVATURE, ELEVATION, AND PACHYMETRIC MAPS

Curvature Maps

There is a high level of agreement between curvature maps obtained from Placido disk-based topography and rotating Scheimpflug tomography (R. Ambrósio, MD, unpublished data, 2009 and 2010; M.W. Belin, MD, unpub-
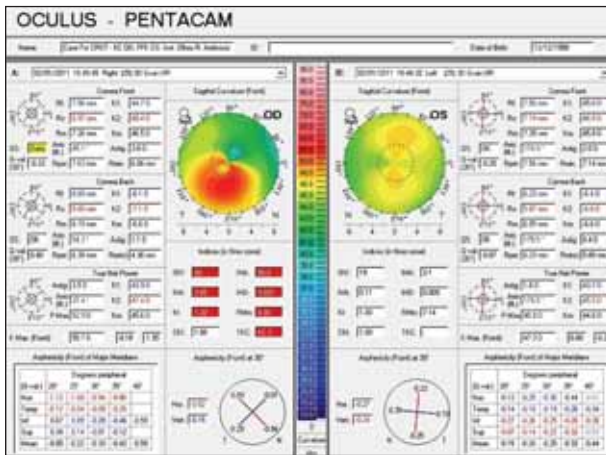
Figure 1. Topometric (front sagittal curvature maps) using the Ambrósio 2 absolute scale from a case with highly asymmetric (not unilateral) keratoconus. Note the topometric keratoconus criteria 2 for the right eye and zero for the left eye.
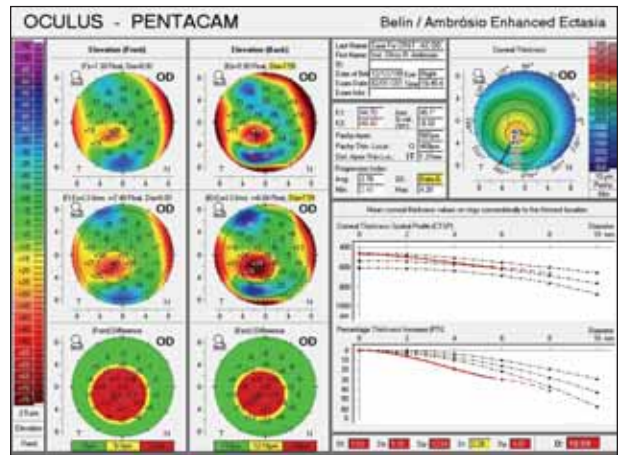

Figure 2. BAD of the right eye of the patient shown in Figure 1. Note the abnormal front and back elevation maps and pachymetric distribution graphs.
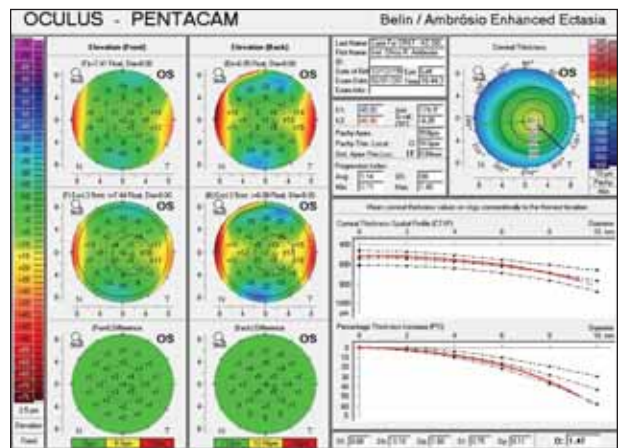

Figure 3. BAD of the left eye of the patient shown in Figure 1. Note the PTI graph, with a deviation from the mean value starting at 5 mm. The BAD deviation value is 1.47. The average PPI is 1.14. The ART average meridian is 450 µm (513 [thinnest point]/1.14 [average PPI]), and the ART maximal meridian is 366 µm (513 [thinnest point]/1.4 [maximal PPI]).

lished data, 2008). Nonetheless, differences are expected because of the fundamental differences between the reflection and projection techniques. The curvature patterns described in normal corneas using Placido disk-based topography[13] are therefore applicable when evaluating Scheimpflug-based corneal tomography, along with the classic criteria for detecting ectasia. The Rabinowitz-McDonnell indices are highly popular. In these, steepness is suspicious when higher than 47.20 D, and superior-inferior asymmetry is suspicious when higher than 1.40 D.[14]

In a normal population (n = 226; R. Ambrósio, MD, unpublished data, 2009), the mean central keratometry reading was 43.10 ±1.43 D (standard deviation [SD]). For the highest keratometry reading, it was 44.60 ±3.40 D (SD). I developed the absolute scale Ambrósio 2, with 61 colors, for curvature maps so that these normal values would be in the range of green to green-blue and the suspicious values would be in the yellow-to-orange range. This scale is also used for pachymetric maps. Artificial intelligence algorithms that employ curvature data can be utilized as the Oculus topometric keratoconus classification as well (Figure 1).

Elevation Maps

Elevation maps are calculated as the difference between the examined corneal surface (anterior or posterior) and a reference body.[15] The best-fit reference with more coincident points is calculated. The geometric body of best fit and the considered area of the corneal surface will influence the elevation map. Both the best-fit sphere (BFS) and the best-fit toric ellipsoid are adequate references for ectasia screening, but different patterns and elevation values will be obtained. For practical purposes, I routinely use the BFS to the fixed area of 8 mm.[12] In normal eyes, an average elevation value at the

thinnest point using a floated BFS for 8 mm is 3.6 ±4.7 µm.[16,17] The best cutoff for keratoconus is 14 µm. The Belin intuitive scale with 61 colors and a 2.5-µm step (Figure 2) has been found to be the most reliable for elevation maps. The yellow value of +15 at the thinnest point warrants suspicion, because it would occur in less than 1% of normal corneas.[18]

Pachymetric Map

The importance of the pachymetric map was once unrecognized. It allows clinicians to determine the truly thinnest point value and its location in relation to the center of the cornea. In addition, it permits characterization of the distribution of thickness throughout the entire cornea.

My colleagues and I have described the concepts of a corneal thickness spatial profile and a percentage thickness increase (PTI) that are displayed in graphs containing the mean and two SD values obtained in a normal population (black dotted lines).[19-21] In addition, pachymetric progression indices (PPIs) are calculated for all hemimeridia over the entire 360° of the cornea, starting from the thinnest point. The PPI will be higher if the cornea abruptly gets thicker from the thinnest point out to the periphery (PTI and corneal thickness spatial profile graphs falling down; Figures 2 and 3). In a normal population, the averages and SD of PPI of the minimal and maximal meridians and the average of all meridians are 0.58 ±0.3, 0.85 ±0.18, and 0.13 ±0.33, respectively.

The PPI is combined with the thinnest point for the calculation of relational thickness. The Ambrósio relational thickness (ART) for the average meridian and the ART maximal meridian are useful for detecting ectasia and ectasia risk. The cutoff values are 480 µm for ART average and 390 µm for ART maximal.

THE BELIN-AMBRÓSIO ENHANCE ECTASIA DISPLAY

The Belin-Ambrósio Enhance Ectasia Display (BAD; Figures 2 and 3) combines the described pachymetric distribution data and the enhanced elevation introduced by Michael W. Belin, MD. In this approach, a new (enhanced) BFS is calculated for the 8-mm zone, excluding an area centered on the thinnest portion of the cornea. If the excluded area protrudes, the resultant BFS will be flatter, and the difference between the standard and enhanced BFS will be high. This approach is used for the anterior and posterior elevations. Normal population studies served as the basis for the green-yellow-red color thresholds on the display.

Deviation of normality values were implemented for the front and back enhanced elevations. Thinnest value, pachymetric distribution, and vertical displacement of the thinnest value in relation to the apex are calculated. In this approach, a value of zero represents the average of the normal population, and a value of one is one SD toward the disease (ectasia) value. A final deviation value is calculated from a regression analysis that weighs each parameter differently. Based on studies involving eyes with normal front curvatures from cases of asymmetric keratoconus, eyes that had ectasia after LASIK with no identifiable risk factors, and eyes that experienced a natural progression of ectasia, my colleagues and I found that a deviation value higher than 1.42 is suspicious for ectasia risk.[12]

CONCLUSION

The detection of ectasia risk among refractive surgery candidates should go beyond corneal topography and CCT. The identification of mild forms of keratoconus and related disorders is not the ultimate goal. Rather, surgeons are attempting to evaluate whether a cornea can biomechanically withstand the refractive procedure. Along with CTm, ophthalmologists should consider performing a corneal biomechanical assessment to increase patients' safety and enhance surgical efficacy. In addition, it is worth taking these novel parameters into account when treating ectatic eyes with alternative procedures to corneal transplantation such as corneal collagen cross-linking, surface ablation, and the implantation of intracorneal ring segments. ■

A video comparing the deformation responses of normal and ectatic corneas is available at http://eyetube.net/?v=rugeg.

Renato Ambrósio Jr, MD, PhD, is the clinical director of cornea and refractive surgery at Instituto de Olhos Renato Ambrósio in Rio de Janeiro, Brazil. He is a consultant to Oculus GmbH. Dr. Ambrósio may be reached at +55 21 2274 5694; renatoambrosiojr@wavefront.com.br.

1. Ambrosio R Jr, Klyce SD, Wilson SE. Corneal topographic and pachymetric screening of keratorefractive patients. *J Refract Surg.* 2003;19(1):24-29.
2. Randleman JB, Russell B, Ward MA, et al. Risk factors and prognosis for corneal ectasia after LASIK. *Ophthalmology.* 2003;110(2):267-275.
3. Randleman JB, Woodward M, Lynn MJ, Stulting RD. Risk assessment for ectasia after corneal refractive surgery. *Ophthalmology.* 2008;115(1):37-50.
4. Randleman JB, Trattler WB, Stulting RD. Validation of the Ectasia Risk Score System for preoperative laser in situ keratomileusis screening. *Am J Ophthalmol.* 2008;145(5):813-818.
5. Randleman JB. Evaluating risk factors for ectasia: what is the goal of assessing risk? *J Refract Surg.* 2010;26(4):236-237.
6. Chan CC, Hodge C, Sutton G. External analysis of the Randleman Ectasia Risk Factor Score System: a review of 36 cases of post LASIK ectasia. *Clin Experiment Ophthalmol.* 2010;38(4):335-340.
7. Klein SR, Epstein RJ, Randleman JB, Stulting RD. Corneal ectasia after laser in situ keratomileusis in patients without apparent preoperative risk factors. *Cornea.* 2006;25(4):388-403.
8. Amoils SP, Deist MB, Gous P, Amoils PM. Iatrogenic keratectasia after laser in situ keratomileusis for less than -4.0 to -7.0 diopters of myopia. *J Cataract Refract Surg.* 2000;26(7):967-977.
9. Ambrosio R Jr, Dawson DG, Salomao M, et al. Corneal ectasia after LASIK despite low preoperative risk: tomographic and biomechanical findings in the unoperated, stable, fellow eye. *J Refract Surg.* 2010:1-6.
10. Binder PS, Trattler WB. Evaluation of a risk factor scoring system for corneal ectasia after LASIK in eyes with normal topography. *J Refract Surg.* 2010;26(4):241-250.
11. Ambrosio R Jr, Belin MW. Imaging of the cornea: topography vs tomography. J Refract Surg. 2010;26(11):847-849.
12. Ambrosio R Jr, Nogueira LP, Caldas DL, et al. Evaluation of corneal shape and biomechanics before LASIK. *Int Ophthalmol Clin.* 2011;51(2):11-38.
13. Rabinowitz YS, Yang H, Brickman Y, et al. Videokeratography database of normal human corneas. *Br J Ophthalmol.* 1996;80(7):610-616.
14. Rabinowitz YS, McDonnell PJ. Computer-assisted corneal topography in keratoconus. *Refract Corneal Surg.* 1989;5(6):400-408.
15. Belin MW, Khachikian SS. An introduction to understanding elevation-based topography: how elevation data are displayed—a review. *Clin Experiment Ophthalmol.* 2009;37(1):14-29.
16. Khachikian SS, Belin MW. Posterior elevation in keratoconus. *Ophthalmology.* 2009;116(4):816, 816.e1; author reply:16-17.
17. Abad JC, Rubinfeld RS, Del Valle M, et al. Vertical D: a novel topographic pattern in some keratoconus suspects. *Ophthalmology.* 2007;114(5):1020-1026.
18. Belin MW, Khachikian SS. An introduction to understanding elevation-based topography: how elevation data are displayed—a review. *Clin Experiment Ophthalmol.* 2009;37(1):14-29.
19. Ambrosio R Jr. Percentage thickness increase and absolute difference from thinnest to describe thickness profile. *J Refract Surg.* 2010;26(2):84-86; author reply:86-87.
20. Ambrosio R Jr, Alonso RS, Luz A, Coca Velarde LG. Corneal-thickness spatial profile and corneal-volume distribution: tomographic indices to detect keratoconus. *J Cataract Refract Surg.* 2006;32(11):1851-1859.
21. Luz A, Ursulio M, Castaneda D, Ambrosio R, Jr. Corneal thickness progression from the thinnest point to the limbus: study based on a normal and a keratoconus population to create reference values [in Portuguese]. *Arq Bras Oftalmol.* 2006;69(4):579-583.